Int. J. Electrochem. Sci., 12 **(2017)** 9626 – 9639, doi: 10.20964/2017.10.80

International Journal of ELECTROCHEMICAL SCIENCE
www.electrochemsci.org

Photovoltaic Performance and Impedance Spectroscopy Analysis of $CuInS_2$ Thin Film Solar Cells Deposited on Polyimide Foil via Spray Pyrolysis

Erkan Aydin and Nurdan Demirci Sankir[*]

Department of Materials Science and Nanotechnology Engineering, TOBB University of Economics and Technology, Ankara, Turkey
[*]E-mail: nsankir@etu.edu.tr, dnurdan@yahoo.com

Received: 16 June 2017 / *Accepted:* 19 August 2017 / *Published:* 12 September 2017

In this study, we have demonstrated that facile, cost-effective and non-vacuum spray pyrolysis technique which is available for fabricating copper indium sulfide ($CuInS_2$) based flexible thin film solar cells for the first time in the literature. First, we have optimized the molybdenum thin films on polyimide foil to obtain proper back contacts via corona surface treatment. The sheet resistivity of the non-treated molybdenum contacts is about 3.7 Ω/□. On the other hand, the sheet resistivity has decreased to 0.8 Ω/□ after corona treatment. The change in the electrical resistivity values of the molybdenum films on polyimide foil has become more effective after post annealing once the samples have been annealed at 300 °C under atmospheric conditions. Therefore, the sheet resistivity of the films after annealing are 2.1 and 258 Ω/□ for corona treated and non-treated samples, respectively. After back contact optimization copper indium sulfide-indium sulfide heterojunctions has been spray pyrolyzed and a novel device structure of polyimide/Mo/CIS/Ag-In_2S_3/ZnO/AZO/Ag/AZO/Ni/Al has been fabricated. Impedance spectroscopy of the solar cell studies revealed that the post annealing of the absorber layer has a pronounced effect on series resistance, parallel resistance, and constant capacitance although it does not cause a significant change in the electron life time. The conversion efficiency of the 1.43% (J_{sc}=10.0 mA/cm^2, V_{oc}=0.52 V, FF=0.37) has been obtained in this work which proved that the facile spray pyrolysis technique is highly beneficial to fabricate flexible solar cells on polyimide substrates. Besides very low chemical precursor consumption, low equipment cost of spray technology and the device structure proposed in this work are some of the key factors while developing the large area flexible solar cells with short energy-payback time.

Keywords: Spray pyrolysis; copper indium sulfide; polyimide; molybdenum; flexible thin film solar cells.

1. INTRODUCTION

Flexible thin film solar cells (Flex-TFSC) have numerous advantages including integration photovoltaics on buildings and uneven surfaces. Moreover, they allow new opportunities in areas such as portable electronics, and space applications [1]. Besides, lightweight, low-cost, robustness and possibility of roll-to-roll deposition make the Flex-TFSC very attractive in many applications where traditional photovoltaic devices cannot compete. Polymer and metal foils can be used as the substrate material for Flex-TFSC. Polymer foils has the advantage of being electrically insulating and thus enable direct monolithic interconnection. Furthermore, unlike the metals, polymer foils are free of metallic impurities that can diffuse into the absorber layer during processing and this adversely affect the electronic properties. On the other hand, the major drawback of the polymer foils is their lower thermal stability compare to the metal foils. Therefore, it is crucial to develop new low-temperature processes for thin film solar cells on polymeric substrates. In this respect, solution-based approaches can potentially be used to realize low cost fabrication of thin film photovoltaics on polymer foils. Although there are large number of studies on vacuum deposition of solar cells on polyimide foils, the number of researches on solution based manufacturing Flex-TFSC on polyimide are very limited [2, 3]. Recently, Möckel et al have been reported the binary Cu–In nanoparticles, Cu–Ga powder and elemental Se nanoparticles containing nanoink formulations on molybdenum coated polyimide via doctor-blade [2]. However, they have not reported a full solar cell structure with photovoltaic performances. Previously, Todorov et al fabricated CIGS absorbers by employing a fully solution based technique [3]. It is important to note that using highly toxic and explosive hydrazine as a solvent is one of the major drawbacks of this technique. On the other hand, spray pyrolysis is also another green chemistry, non-vacuum and low temperature technique. This technique allows to high material utilization with very low solution consumption [4]. Previously thin films of zinc oxide [5], copper/silver [6], fluorine-doped tin oxide [7], indium oxide [8], and indium tin oxide [9] have been deposited on polyimide substrates via spray pyrolysis technique. Besides spray pyrolysis of the copper indium sulfide ($CuInS_2$) based solar cells on glass have been extensively studied [10-14]. According to our best knowledge there is no report on manufacturing of chalcopyrite solar cell on flexible polymer substrates via spray pyrolysis technique. In this study, we have fabricated $CuInS_2$-based thin film solar cells on polyimide films employing spray pyrolysis technique without using any toxic process steps. Optical, morphological, structural and electrochemical properties of the as-deposited and thermally annealed $CuInS_2$ absorber layer deposited on polyimide have been investigated. Additionally, impedance spectroscopy has been studied to investigate the full solar cell device structure.

2. EXPERIMENTAL

2.1. Preparation and Characterization of Molybdenum Back Contacts

Molybdenum back contacts are prepared on polyimide foils (125 μm-thick Upilex®) in two steps. In the first step, corona surface treatment has been applied on Upilex® foils for 10 s prior to the molybdenum deposition by using Enercon Dyne-A-Mite™ HP Air Plasma Surface Treater. Before the deposition of molybdenum, samples are heated to 200 °C for 30 min. Then, the first layer of

molybdenum films has been deposited by magnetron sputtering system (Vaksis Midas 2M2T RF). RF power density was 6.2 Wcm^{-2} and processing time is 15 minutes, which results 225 nm-thick films.

In the second step, 10 s microwave (2.45 Ghz) Ar plasma treatment is applied to the molybdenum coated Upilex® foils at 650 W power and another 225 nm-thick molybdenum films are further deposited. After the deposition of back contacts samples are allowed to cool down naturally to room temperature. Wettability of Upilex® foils is examined by contact angle measurement system (OCA 30, Dataphysics). Sheet resistivity of back contacts is measured using Lucas Lab 4-point probe system equipped with Keithley 2400 Sourcemeter. The adhesion test is performed using cross hatch tape adhesion test (hatch cutter) with Cross Cut Adhesion Tester (Biuged Laboratory Instruments) and ASTM D3359-B with 1 mm spacing.

2.2. Preparation and characterization of $CuInS_2$ absorber layers and photovoltaic devices

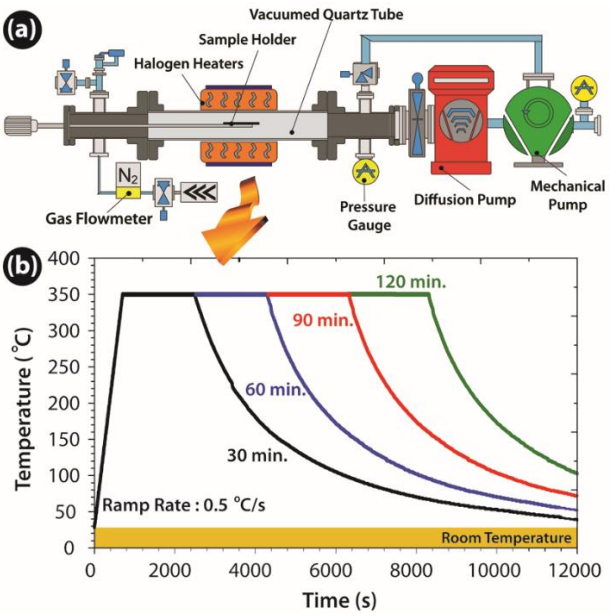

Figure 1. (a) Schematic illustration of rapid thermal annealing system and (b) temperature course of annealing processes. (temperature values were measured from the surface of the samples and all annealing procedures were conducted under nitrogen environment after $1x10^{-6}$ Torr base pressure)

$CuInS_2$ absorber layers have been deposited on molybdenum thin films using spray pyrolysis (Sono-Tek FlexiCoat USP System) technique. Detailed information about the coating system and the unique mist generation technology has been reported in our preceding study [15]. Aqueous solution containing 9.4 mM Copper (II) chloride-dehydrate ($CuCl_2$, Sigma-Aldrich), 5.5 mM indium (III) chloride ($InCl_3$, Sigma-Aldrich), and 16 mM thiourea (NH_2CSNH_2, Sigma-Aldrich) is sprayed using N_2 as a carrier gas. Deposition of $CuInS_2$ films is performed on molybdenum coated Upilex® foils heated at 300 °C. Post annealing process has been performed in Vaksis CVD-Handy/Tube RTA halogen lamp furnace with a quartz tube as reaction chamber (Fig.1). Samples are annealed at 350 °C

under nitrogen environment for a time interval ranging between 30 to 120 min. The as deposited and annealed samples are processed into photovoltaic device, using methods including spray pyrolysis of In_2S_3 (~0.95 µm), RF sputtering of i-ZnO (~50 nm) and AZO+Ag+AZO sandwich TCO structures (~110 nm) and thermal evaporation of Ni/Al grids as defined our early study [16]. The crystal structure of the films is analyzed via using Panalytical X'pert Pro MPD X-ray diffractometer (CuK_α, λ= 1.5405 Å). The surface morphology analysis and thickness measurement of the thin films are performed by FEI, Quanta 200 FEG scanning electron microscopy (SEM). Dispersive X-Ray Analysis (EDX) is used to determine the elemental composition of the films at 15 kV accelerating voltage. Raman spectra are obtained by excitation using argon ion and diode lasers (Horiba Jobin Yvon Model: IHR550). J-V characteristics of the fabricated solar cells are measured in the dark and under AM 0 illumination. Solar cells have been illuminated using Lot-Oriel solar simulator with 150W Xenon short arc lamb mounted AM 0 filter. AC conductivity of the films is implemented at room temperature using a Solartron SI 1260 Impedance/Gain-Phase Analyzer equipped with a SI1287 Electrochemical Interface.

3. RESULTS AND DISCUSSION

3.1. Molybdenum thin film back contacts on Upilex® foils

It is well-known fact that properties of back contacts have a crucial role on the performance of thin film solar cells. Hereby, improving the adhesion characteristics on the substrate and electrical resistivity of molybdenum are very important two parameters for obtaining high quality back contacts. Metallization of polyimide substrates is a hard topic due to the hydrophobic nature of it. Hence, surface modification by adding chemically active groups is unavoidable. In literature, chemical methods such as sodium hydroxide (NaOH) and potassium hydroxide (KOH) treatment and sulfonation have been commonly used for the modification of polyimide surface before metallization [17, 18]. Here we preferred atmospheric corona treatment method which is due to being a cost effective and rapid process to improve the molybdenum-Upilex® interface for thin film deposition applications. This method has been successfully applied on polyimide foils by Ogawa et al and Eom et al [19, 20]. On can easily notice that plasma treatment leads to the bond scission of imide groups to form carbonyl and secondary amide groups. Hence, after corona treatment the surface of the Upilex® films have changed from hydrophobic to hydrophilic. As can be seen in Fig. 2a. wettability of the Upilex® surface remarkably has improved after corona treatment. Contact angle measurements also affirms that surface energy of Upilex® substrates has drastically increased after corona treatment (Fig. 2b.). Contact angle of treated surface is 18º while it is measured as 80º for non-treated Upilex®.

In order to form back contact, molybdenum thin films have been deposited on both corona treated and non-treated polyimide foils via magnetron sputtering. The annealing process at 300 °C in ambient atmosphere has been applied to all molybdenum coated Upilex® foils to mimic the experimental conditions of the absorber layer deposition on top of the back contact. Fig 3a and b show the optical microscopy images of molybdenum films on Upilex®. Without corona treatment, the density and the depth of the cracks formed on the surface is higher than that of the corona treated polyimide foils. In other words, the crack density has been remarkably reduced via corona treatment.

The large mismatch between the coefficient of thermal expansion (CTE) values of substrate and coated films generally results with cracking and debonding of the coating. CTE values of Mo and Upilex® are 4.8-5.9 and 12-24 (10^{-6} K^{-1}), respectively [21]. The difference in the CTE of molybdenum and Upilex® is caused a stress in the interface resulting the crack formation on the surface. Corona treatment also affects the results in the XRD spectra of the molybdenum films (Fig. 3c). It has been observed that the molybdenum films have cubic structure (JCPDS 42-1120) with two main peaks around 40.7° (2θ) and 74°(2θ). The intensities of these peaks have been increased after corona treatment, indicating the improvement of the crystallinity.

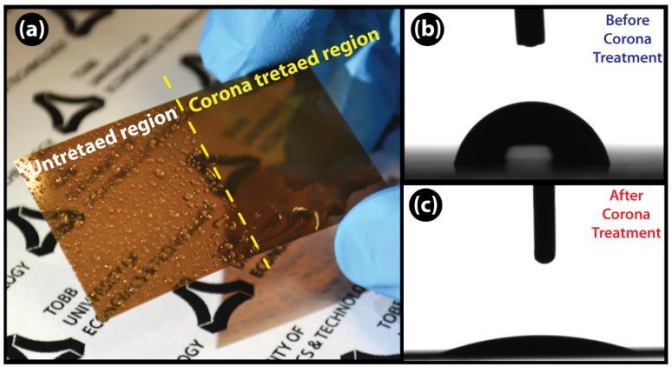

Figure 2. (a) Photograph illustrating the difference of wettability (water) before and after corona treatment process on Upilex® foils. Contact angle measurements (b) before and (c) after corona treatment process.

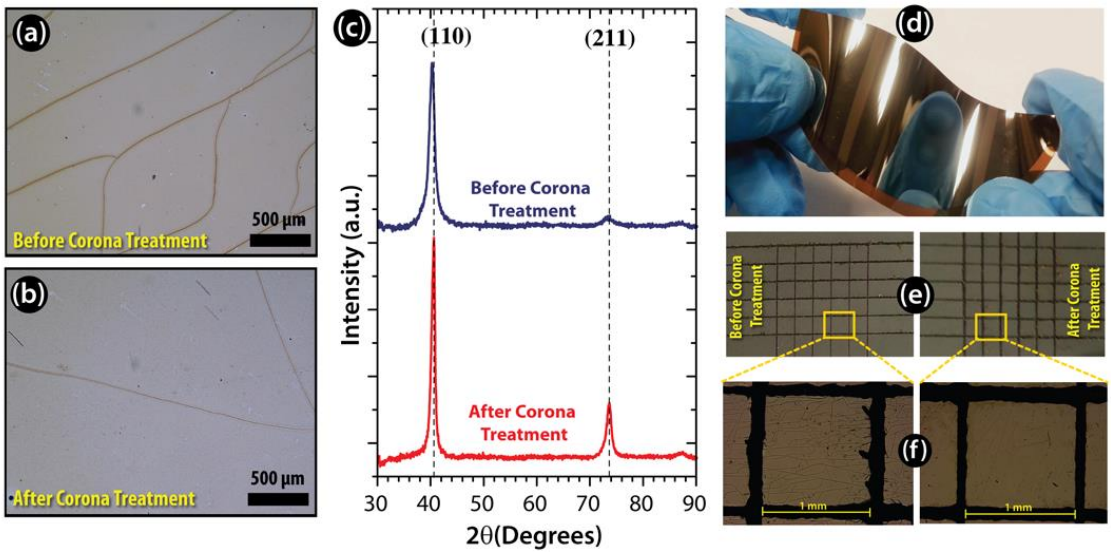

Figure 3. Optical microscopy images of the molybdenum films before (a) and after (b) corona treatment (samples are annealed at 300 °C in order to mimic pyrolysis process) and (c) XRD spectra of molybdenum films before and after corona treatment. **(**d) Photographs of molybdenum films coated on corona treated flexible Upilex® foils and (e) after cross-hatch adhesion test. (f) Optical microscopy images of cross-hatch squares.

The adhesion properties of the molybdenum films have been analyzed qualitatively by cross-hatch adhesion tester. Fig. 3e and Fig. 3f show the photographs and optical microscopy images of molybdenum films after cross-hatch test, respectively. Accordingly, non-treated samples result with adhesion failure less than 5% according to ASTM D3359-B Standards. On the other hand, no failure behavior has been observed for the corona treated samples. Adhesion and the crack formation directly influence the electrical conductivity of the molybdenum films. 4-point probe measurements reveal that the non-treated samples have 3.7 Ω/□ sheet resistivity. This value decreases to 0.8 Ω/□ for the molybdenum films deposited on the corona treated polyimide foils. A more pronounced change in the electrical resistivity has been observed after annealing process. In accordance with the increased crack density sheet resistivity of the non-treated samples reaches to 258 Ω/□ after annealing process, although the sheet resistivity of the corona treated samples are only 2.1 Ω/□. This means that the corona treatment certainly helps to decrease crack density and also electrical resistivity. Hence molybdenum back contacts deposited on corona treated polyimide are able to tolerate for high temperature atmospheric deposition conditions required for spray pyrolysis process.

3.1. Properties of $CuInS_2$ films

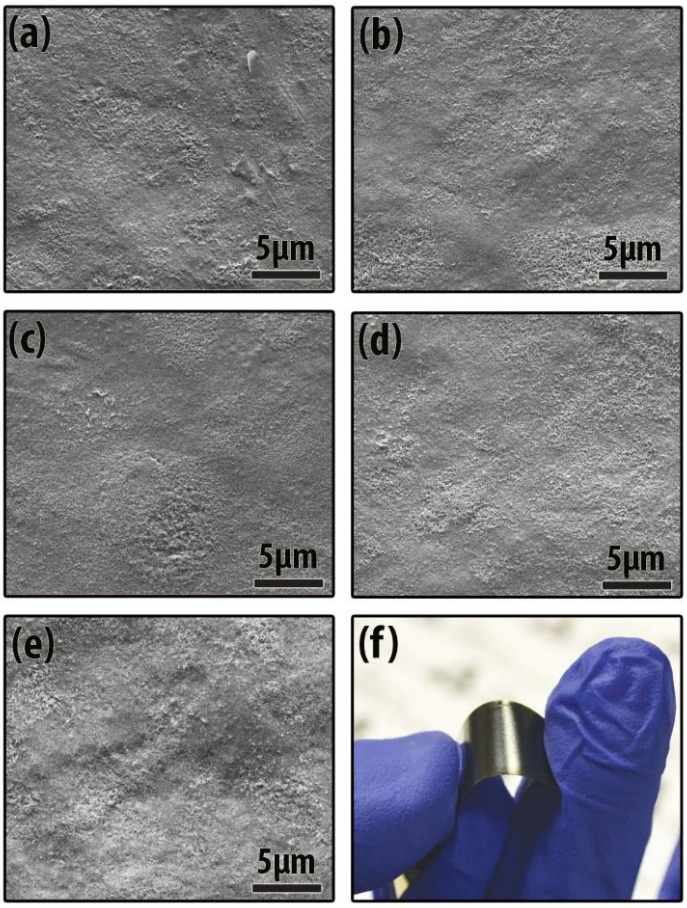

Figure 4. Top-view SEM images of (a) as deposited, (b) 30 min., (c) 60 min., (d) 90 min. annealed $CuInS_2$ thin films. (f) Photograph of the bended $CuInS_2$ thin films on molybdenum coated Upilex® foils.

Surface quality of the $CuInS_2$ films has been investigated by SEM analysis. Fig. 4 shows SEM surface morphology images of 25μm x 25μm part of $CuInS_2$ thin films on molybdenum coated Upilex® foils with different annealing periods. As can be seen on Fig. 4 all sprayed and annealed films have no cracks, surface defects or pin-holes. Therefore, it can be concluded that studied pyrolysis and annealing temperatures well suit for the formation of high quality $CuInS_2$ films on Upilex® foils. Pyrolytic growth of all $CuInS_2$ crystals is evident from the dominant (112) plane at 28° (2θ) value of XRD patterns in Fig. 5. Moreover, the diffraction peaks at 30.4°, 46.4°, 55.1°, 57.7° and 74° (2θ) values are reflections from (004)/(200), (204)/(220), (116)/(312)/(215), (224) and (136) crystal planes of $CuInS_2$, respectively. Besides, the observed sharp peak at 40.5° (2θ) most probably belongs to the (100) plane of molybdenum, which is used as the back contact (JCPDS 42-1120). Furthermore, very minor peaks observed between 20-25° (2θ) is probably due to the peaks from Upilex® foils (Fig. 5).

All samples possess nanocrystalline structure as calculated from the well-known Debye-Scherrer formula with a 0.89 correction factor. Moreover, the crystallite size of the films, which is in the range of 27-34 nm, has not drastically changed with chosen annealing periods because of low annealing temperature of 350°C used here.

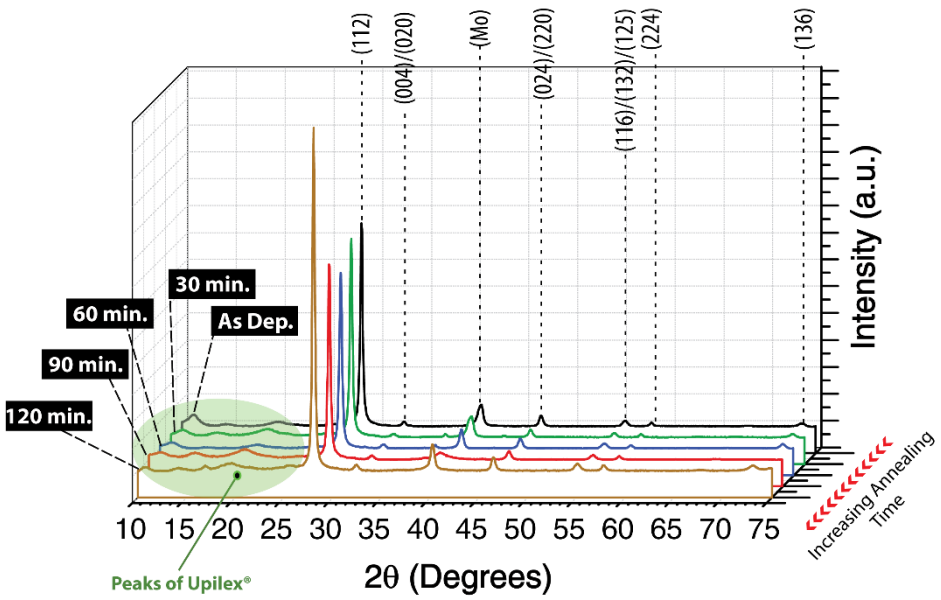

Figure 5. X-ray diffraction spectra of as deposited and annealed $CuInS_2$ thin films on Upilex® foil.

Raman spectroscopy measurement has been performed at room temperature to further check the crystal quality and phase purity of the films (Fig. 6). All sprayed films have showed a dominant A_1 phonon mode at 305 cm^{-1} which indicates $CuInS_2$ phase [22]. The broad A_1 mode shows the amorphous nature of the processed films validating the XRD data. The spray processed and annealed samples have the broad peaks at 280–310 cm^{-1} indicates the mixed CH and CA-ordering [23]. The observed shoulder peaks at 240 cm^{-1} ($E3^{TO}$, $B_2{}^2{}_{TO}$) and 340 cm^{-1} ($E^1{}_{LO}$) bears the Raman modes for CH ordering [24]. It is noteworthy to mention here that, the most favorable secondary phases during the spray pyrolysis process of $CuInS_2$ are CuS and Cu_2S which have dominant vibration modes at 474

and 472 cm^{-1} respectively [25]. However, no impurity phase is detected on Raman spectra of the processed films.

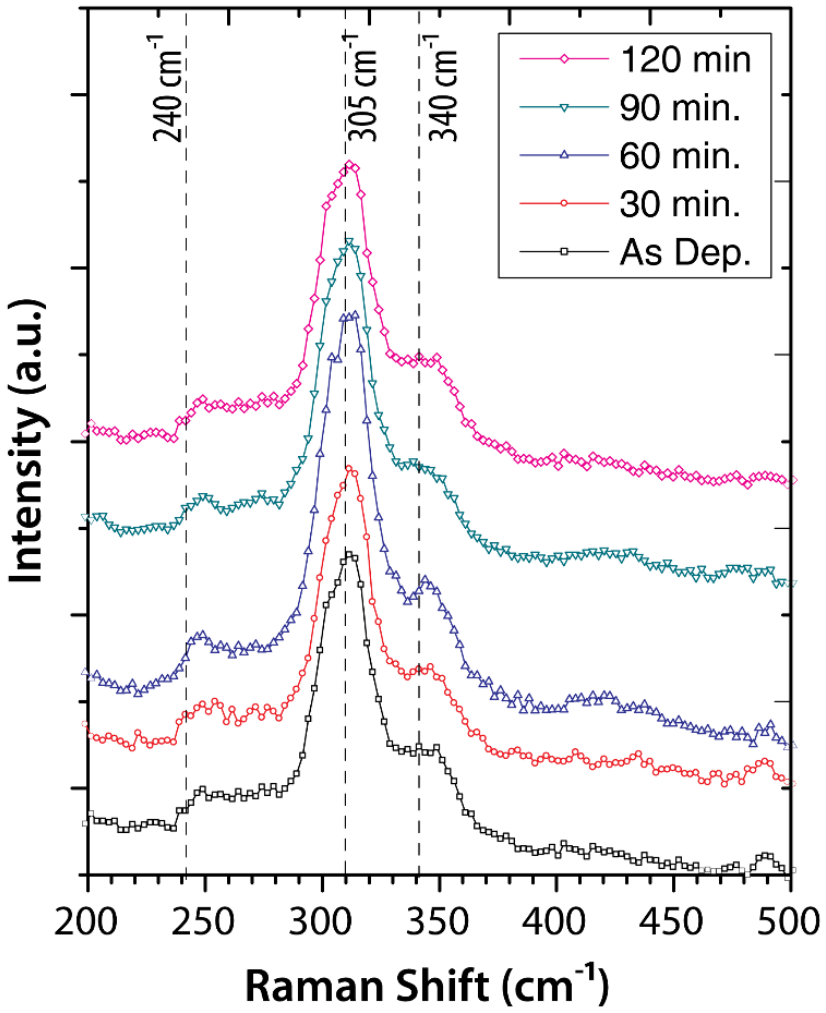

Figure 6. Raman spectra of as deposited and annealed $CuInS_2$ thin films on Upilex® foil.

3.3. Cell configuration and photovoltaic characteristics

The as deposited and annealed $CuInS_2$ films are then processed into solar cells with the structure of Upilex®/Mo/$CuInS_2$/Ag-In_2S_3/i-ZnO/AZO-Ag-AZO/Ni-Al without an antireflection coating (Fig. 7a.). To form a p-n junction, we have deposited 0.95 µm silver doped In_2S_3 thin films deposited on as deposited on post-annealed $CuInS_2$ films as explained in preceding study [26]. Our previous studies have shown that, silver incorporation improves the electro-optical properties of the In_2S_3 films drastically [26, 27]. Hence, we prefer 1% silver doping ratio for the deposition of buffer layer as an optimized value. Fig. 7b. shows the schematic device structure and the cross-sectional SEM images of best performed device on flexible foil can be seen in Fig. 7c. Additionally, well-defined layers of back contact, absorber, buffer and TCO thin films can obviously be seen in the same figure.

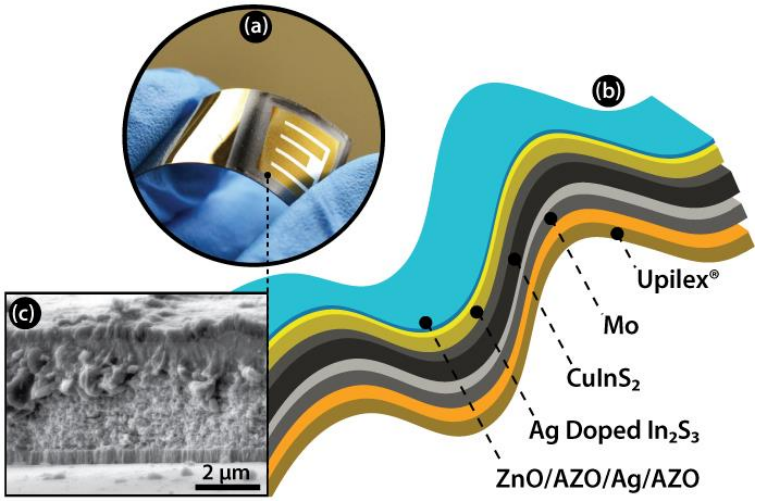

Figure 7. (a) Photographs, (b) schematic illustration and (c) cross section SEM images of fabricated device structure.

For the completed solar cell structures the current density as a function of voltage has been studied (Fig. 8). Moreover, photovoltaic performances from typical light J-V curves are summarized in Table 1. Apparently, if the post annealing process is not applied on $CuInS_2$ thin films we faced with short behavior on the junction. However, in accordance with the raised annealing period up to 90 min photovoltaic parameters such as short circuit current density (J_{sc}), open circuit voltage (V_{oc}) and efficiency (η) values have been improved. The maximum solar cell efficiency is 1.43% once the samples have been annealed for 90 min. However, further increasing the annealing periods to 120 min has caused deterioration on the photovoltaic parameters (Table 1).

Table 1. Some of the photovoltaic parameters of $CuInS_2$ based devices.

Sample	**V_{OC} (V)**	**J_{SC} (mA/cm^2)**	**FF**	**η (%)**	**R_S (Ω)**	**R_{SH} (Ω)**
As Dep.	-	-	-	-	-	-
30 min.	0.46	3.88	0.32±0.06	0.41±0.03	209.02	$1.00x10^3$
60 min.	0.50	4.74	0.31±0.05	0.55±0.04	160.96	$1.29x10^3$
90 min.	0.52	10.0	0.37±0.01	1.43±0.11	93.58	$1.11x10^4$
120 min.	0.35	3.13	0.30±0.07	0.24±0.02	307.95	$1.00x10^3$

It is believed that the low FF values (max. 37%) most likely is resulted from recombination of photoexcited electrons at grain boundaries. The recombination is evident in the low value of the shunt resistance, $R_{sh}=(dV/dI)_{V=0}$, in the J–V characteristic recorded under illumination. Previously, Oh et al has reported similar FF values for sol-gel processed $Cu(In,Ga)S_2$ solar cells on flexible Upilex® foils [28]. Post annealing of $CuInS_2$ films with increased annealing period up to 90 min typically increases R_{sh} by a factor of 10 and decreases R_s by factor of 2 (Table 1). However, still we have high R_s values most probably due to the large grain boundaries arising from fine grains. In order to increase the grain

size, one can anneal the samples at higher temperatures. Nonetheless, this will cause in the degradation of the substrate due to the relatively low glass transition temperature of the polyimide. Table 2 summarizes the structures, photovoltaic and key experimental parameters of the spray pyrolyzed $CuInS_2$ thin film solar cells on glass substrates. As can be seen in this table our photovoltaic parameters are comparable with literature. Besides our work has the advantages of using flexible substrate. Moreover, it is important to emphasize here that we do not use any toxic material like H_2S gas and doping process to improve the performance of the absorber layer.

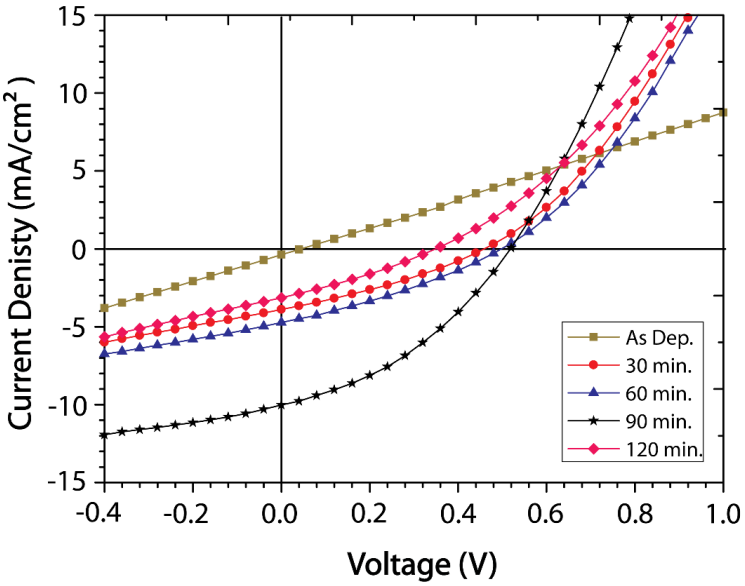

Figure 8. Characteristic J-V graphs (under illumination) of thin film solar cells having Upilex®/Mo/$CuInS_2$/Ag-In_2S_3/i-ZnO/AZO-Ag-AZO/Ni-Al structure.

To have a deeper insight into the influence of annealing periods on the photovoltaic parameters room temperature impedance measurements have been performed for the thin film solar cells having Upilex®/Mo/$CuInS_2$/Ag-In_2S_3/i-ZnO/AZO-Ag-AZO/Ni-Al structure. Fig. 9a. shows a typical EIS spectrum of the fabricated devices. Impedance data are taken at a DC bias of 0 V and an AC voltage of 25 mV at 1 Hz-100 kHz frequency range. For analyzing and fitting of the electrical impedance data Z-View software (Scribner Associates) is used. The spectrum shows a single semicircle which is evident of single relaxation process. The radii of the semicircles tend to increase with increasing annealing period. An equivalent circuit of heterojunctions broadly be made up of three elements: a series resistance (R_s), parallel resistance (R_p), and constant capacitance (C) or "capacitance-like element" called a constant phase element (CPE) [29]. In our case, an equivalent circuit with R-C elements (Fig. 9b.) is employed to fit the EIS data with low error values. From EIS, it is possible to extract the series resistance (R_s) and the charge recombination resistance (R_p) in the cell. The semicircle intersection with the abscissa in high frequency region depends on the series resistance.

Table 2. Structure, photovoltaic and some key experimental parameters of $CuInS_2$ based thin film solar cells deposited on glass via spray pyrolysis method.

Solar cell structure	Photovoltaic paremeters	Notes	Ref.
FTO/$CuInS_2$/In_2S_3/Ag	η= 0.94%, FF=38%, V_{oc}=457mV, J_{sc}=5.45mAcm^{-2}	$CuInS_2$, In_2S_3 and fluorine doped tin oxide (FTO) thin films are deposited via spray pyrolysis. Deposition temperature and spray volume for $CuInS_2$ thin films are fixed at 350 °C and 80 ml, respectively.	[10]
F-doped SnO_2/TiO_2/In_2S_3/$CuInS_2$/Mo	η=1.7%, FF=35% V_{oc}=370 mV, J_{sc}=11.2 mAcm^{-2}	The $CuInS_2$ films, In_2S_3 buffer and TiO_2 compact layers are deposited by the spray method. However, the repeatability of the best cell is rather low.	[11]
ITO/$CuInS_2$/In_2S_3/Ag	η= 2.13%, FF=30%, V_{oc}=466 mV J_{sc}=14.8 mAcm^{-2}	$CuInS_2$/In_2S_3 layers are deposited via spray pyrolysis (Cu/In ratio in the $CuInS_2$ is 1/1 and In/S ratio in the In_2S_3 layer is 1.2/12)	[12]
FTO/TiO_2/In_2S_3/$CuInS_2$	η=2.88% FF=45% V_{oc}=551 mV, J_{sc}= 11.65 mAcm^{-2}	$CuInS_2$ (CIS) films were deposited on In_2S_3/TiO_2/FTO/glass under air by spray pyrolysis (The best cells are achieved at 4% sodium doping using 350°C hot–plate)	[13]
Al:ZnO/CdS/CIS(or Ga:CIS)/Mo	η=5.8%, FF=54% V_{oc}=730mV, J_{sc}=14.6 mAcm^{-2}	The best performed cell is obtained from the gallium doped $CuInS_2$ thin films annealed at 600°C in sulfur rich environment.	[14]
Upilex®/Mo/$CuInS_2$/Ag-In_2S_3/i-ZnO/AZO-Ag-AZO/Ni-Al	η=1.43%, FF=37% V_{oc}=520mV, J_{sc}=10.0 mAcm^{-2}	$CuInS_2$/Ag-In_2S_3 thin films have been deposited via spray pyrolysis. CuInS2 films have been annealed at 90°C in nitrogen environment	This work

Circuit parameters have been calculated from the fitting values obtained via Z-View software and summarized in Table 3. Additionally, R_s fitting values are also provided in Table 3. As can be seen in Table 3, R_s values indicating the contact resistances are all in ohm range. This is a sign for the efficient charge collection through the ohmic contacts. Interestingly the R_s value of the 120 min

annealed samples increase and reaches up to approximately 18 Ω, which is higher than the R_s value of as-deposited samples.

Table 3. Some important parameters of $CuInS_2$ based devices obtained by impedance spectroscopy and capacitance-voltage analysis.

Sample	R_S (Ω)	R_P (Ω)	C (F)
As Dep.	17,2± %2.8	222.3± %0.5	$8.6x10^{-9}$ ± %1.2
30 min.	17.5 ± %3.7	347.8± %0.8	$1.1x10^{-8}$ ± %1.6
60 min.	12.2 ± %7.1	545.8± %0.6	$9.3x10^{-9}$ ± %1.1
90 min.	12.7 ± %9.1	934.1± %0.8	$1.3x10^{-10}$ ± %1.4
120 min.	17.9 ± %9.4	1521± %1.1	$1.7x10^{-10}$ ± %1.6

Therefore, the decrease in photovoltaic efficiency observed for this sample can be attributed to the increase in the R_s. Moreover, in accordance with the annealing period, R_p values increases. As shown in the Bode plot, the peak frequency is slightly shifted from high frequency to low frequency with the addition of the blocking layer. These data are in coincidence with the previously reported studies on annealing effects on the impedance spectroscopy of photovoltaic devices [30].

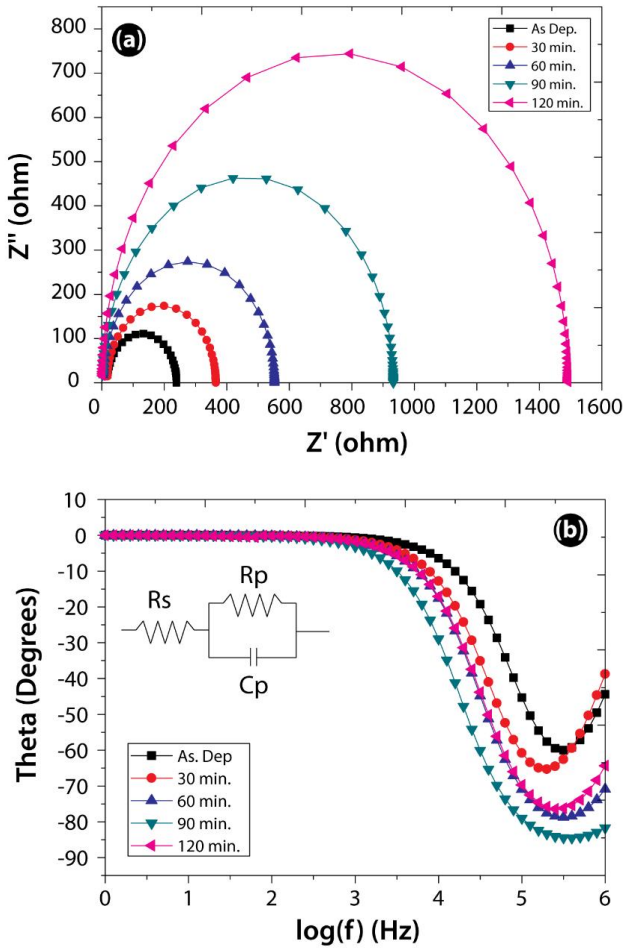

Figure 9. (a) Nyquist and (b) Bode phase plots of $CuInS_2$ based devices. Impedance data were collected under a bias of 0 V and under dark conditions.

4. CONCLUSIONS

In summary, novel flexible thin film solar cells have been successfully fabricated on Upilex® foils using a simple spray pyrolysis method. The use of corona treatment makes the molybdenum thin films more adherent on the surface of Upilex®. Moreover, sheet resistivity of the molybdenum thin films deposited on the corona treated Upilex®, is much lower than the molybdenum thin films deposited on un-treated samples. It is observed that annealing period has a critical role on the efficiency of spray pyrolyzed solar cells. Although the J−V curves of solar cell structures with as-deposited $CuInS_2$ absorber layer apparently include poor properties, an appreciable solar cell property for the solution processed solar cell with η of 1.43% is obtained for 90 min annealed samples. Reported J_{sc}, V_{oc} and FF values in this work are comparable with literature and shows the potential to use our structure in large scale and ecofriendly flexible thin film solar cell applications.

References

1. A. Chirilă, P. Reinhard, F. Pianezzi, P. Blöesch, A.R. Uhl, C. Fella, L. Kranz, D. Keller, C. Gretener, H. Hagendorfer, D. Jaeger, R. Erni, S. Nishiwaki, S. Buecheler and A.N. Tiwari, *Nat. Mater.* 12 (2013) 1107.
2. S.A. Möckel, T. Wernicke, M. Arzig, P. Köder, M. Brandl, R. Ahmad, M. Distaso, W. Peukert, R. Hock and P.J. Wellmann, *Thin Solid Films* 582 (2015) 60.
3. T. K. Todorov, O. Gunawan, T. Gokmen and D. B. Mitzi, *Prog. Photovoltaics* 21 (2013) 82.
4. N. D. Sankir, E. Aydin, H. Unver, E. Uluer and Parlak, M., *Sol. Energy* 95 (2013) 21.
5. M. G. Faraj and P. Taboada, *J. Inorg. Organomet. Polym.* (2017) DOI 10.1007/s10904-017-0594-9
6. S. Suren, W. Limkitnuwat, P. Benjapongvimon and S. Kheawhom, *Thin Solid Films* 607 (2016) 36.
7. A. Muthukumar, G. Giusti, M. Jouvert, V. Consonni and D. Bellet, *Thin Solid Films* 545 (2013) 302.
8. L. Petti, H. Faber, N. Münzenrieder, G. Cantarella, P. A. Patsalas, G. Tröster, and T. D. Anthopoulos, *Appl. Phys. Lett.* 106 (2015) 092105.
9. R. Rana, J. Chakraborty, S. K. Tripathi, M. Nasim, *J. Nanostruct. Chem.* 6 (2016) 65.
10. M.V. Santhosh, D.R. Deepu, C. Sudha Kartha, K. Rajeev Kumar, K.P. Vijayakumar, *Sol. Energy* 108 (2014) 508.
11. S. Lugo, I. López, Y. Peña, M. Calixto, T. Hernández, S.Messina and D. Avellaneda, *Thin Solid Films* 569 (2014) 76.
12. A. S. Cherian, T. Abe, Y. Kashiwaba, C. Sudha Kartha and K.P. Vijayakumar, *Enrgy. Proced.* 15 (2012) 283.
13. D-C Nguyen, T. Ryo, L. Lombez and S. Ito, *Int. J. Nanotechnology,* 10 (2013) 279.
14. S. Ikeda, M. Nonogaki, W. Septina, G. Gunawan, T. Harada and M. Matsumura, *Catal. Sci. Technol.*, 3 (2013) 1849.
15. N. D. Sankir, E. Aydin, M. Sankir and A. Bozbey, *J. Mater. Process. Tech.* 214 (2013) 1879.
16. N. D. Sankir, E. Aydin, E. Ugur and M. Sankir, *J. Alloy. Compd.* 640 (2015) 468.
17. N. D. Sankir and R. O. Claus, *J. Mater. Process. Tech.* 196 (2008) 155.
18. E. Ranucci, A. Sandgren, N. Andronova and A. C. Albertsson, *J. Appl. Polym. Sci.*, 82 (2001) 1971.
19. T. Ogawa, S. Baba and Y. Fujii, *J. Appl. Polym. Sci.* 100 (2006) 3403.
20. J. S. Eom and S. H. Kim, *Thin Solid Films* 516 (2008) 4530.
21. F. Kessler and D. Rudmann, *Sol. Energy* 77 (2004) 685.

22. J. Alvarez-Garcia, A. Perez-Rodrıgueza, A. Romano-Rodriguez, T. Jawhari, J. R. Morante, R. Scheer and W. Calvet, *Thin Solid Films* 387 (2001) 216.
23. D.Y. Lee and J.H. Kim, *Thin Solid Films* 518 (2010) 6537.
24. W. H. Koschel and M. Bettini, *Phys. Status Solidi B* 72 (1975) 729.
25. B. Minceva-Sukarova, M. Najdoski, I. Grozdanov and C. J. Chunnilall, *J. Mol. Struct.* 410-411 (1997) 267.
26. N. D. Sankir and E. Aydin, *Int. J. Electrochem. Sci.* 9 (2014) 3864.
27. E. Aydin, M. Sankir, N. D. Sankir, *J Alloy. Compd.* 603 (2014) 119.
28. Y. Oh, K. Woo, D. Lee, H. Lee, K. Kim, I. Kim, Z. Zhong, S. Jeong and J. Moon, *ACS Appl. Mater. Interfaces* 6 (2014) 17740.
29. M. Sugiyama, M. Hayashi, C. Yamazaki, N. B. Hamidon, Y. Hirose, M. Itagaki, *Thin Solid Films* 535 (2013) 287.
30. H. Wang, S. Yang, Y. Wang, J. Xu, Y. Huang, W. Li, B. He, S. Muhammad, Y. Jiang, Y. Tang, B. Zou, *Org. Electron.* 42 (2017) 309.